# Internal Barrier Discharges in JET and their Sensitivity to Edge Conditions

The JET Team[1] (prepared by A.C.C. Sips 1)

JET Joint Undertaking, Abingdon, Oxon, OX14 3EA, United Kingdom.
1) Present address: Max-Planck-Institut für Plasmaphysik, EURATOM Asssoziation, Boltzmannstrasse 2, D-85748, Garching, Germany.

e-mail contact of main author: ccs@ipp.mpg.de

**Abstract.** Experiments in JET have concentrated on steady state discharges with internal transport barriers. The internal transport barriers are formed during the current rise phase of the discharge with low magnetic shear in the centre and with high additional heating power. In order to achieve stability against disruptions at high pressure peaking, typical for ITB discharges, the pressure profile can be broadened with a H-mode transport barrier at the edge of the plasma. However, the strong increase in edge pressure during an ELM free H-mode weakens the internal transport barrier due to a reduction of the rotational shear and pressure gradient at the ITB location. In addition, type I ELM activity, associated with a high edge pedestal pressure, leads to a collapse of the ITB with the input powers available in JET. The best ITB discharges are obtained with input power control to reduce to core pressure, and with the edge of the plasma controlled by argon gas dosing. These discharges achieve steady conditions for several energy confinement times with H97 confinement enhancement factors of 1.2-1.6 at line average densities around 30%-40% of the Greenwald density. This is at much lower density (typically factor 2 to 3) compared to standard H-mode discharges in JET. Increasing the density, using additional deuterium gas dosing or shallow pellet fueling has not been successful so far. A possible route to higher densities should maintain the type III ELM's towards high edge density, giving scope for future experiments in JET.

## 1. Introduction

Regimes with Internal Transport Barriers (ITB's) provide a route for enhanced performance in Tokamak experiments. In the past few years, research has concentrated on heating during the current rise phase of the discharge in conditions of weak or reversed magnetic shear in the centre. In JET, experiments on internal transport barriers were started during the Mark IIa divertor campaign (1996/1998) [1,2]. Since 1999, the experiments are performed with the Mark II Gas Box divertor, a more closed divertor compared to Mark IIa. During this phase the experiments have focussed on the formation of internal transport barriers and the development of the ITB discharges towards steady state.

In this paper the conditions for sustaining ITB's with an H-mode edge in JET are presented. After an introduction, the barrier evolution during the formation of an ELM free H-mode and the subsequent type I ELM activity is given. It is show that input power control and a control of the edge pressure with impurity seeding are required to maintain the ITB discharges for several energy confinement times. Finally, the confinement of these discharges and the edge conditions required to sustain the ITB's are compared to standard H-mode discharges in JET.

## 2. Internal Transport Barrier's in JET

The optimum condition for the formation of internal barriers in JET, is a plasma with low shear in the centre and $q_{axis}$ values close to 2 [3]. This can be obtained with a current rise (0.4 MA/s) in X-point at low density. LHCD can be used as breakdown assist (optional), low power (~ 1 MW) ICRF with the H-minority heating in the centre is used as preheating. High

[1] A list of the JET Team is given in OV1/2 by C. Gormezano.

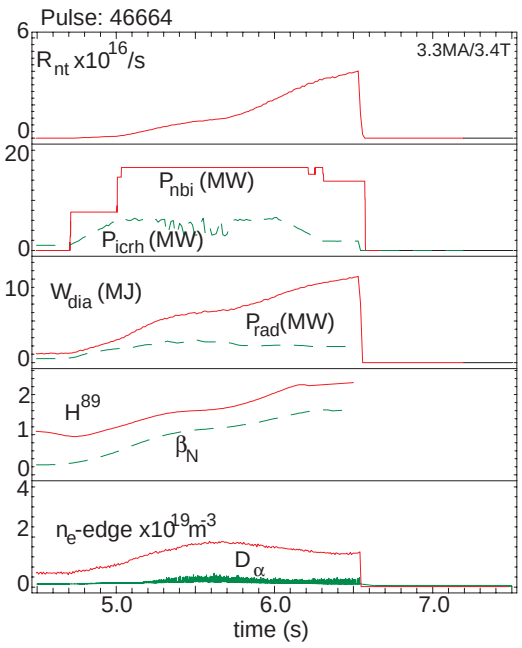


*Fig. 1. The formation and evolution of an ITB at 3.3MA/3.4T. NBI and ICRF heating is applied during the current ramp phase of the discharge. The ITB is formed at 5.8 seconds as deduced from the rapid rise of the neutron rate ($R_{nt}$) and stored energy ($W_{dia}$). The dischargedisruptions, despite a reduction of the input power.*

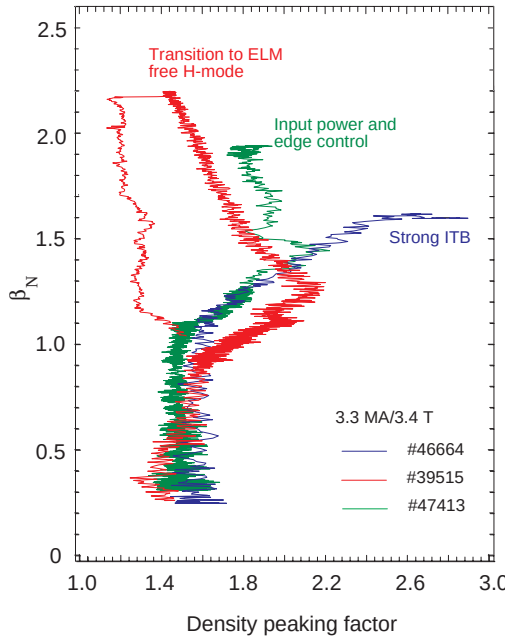


*Fig. 2. The evolution of the density peaking $n_{e0}/<n_e>$ for 3 ITB discharges. The profiles continue to peak for pulse 46664 (see Fig. 1). This profile peaking can be reduced with a transition to an ELM free H-mode (pulse 39515) or with control of the input power in combination with edge control (pulse 47413).*

power is applied at low target density ($n_{e0}$ ~$0.6\cdot10^{19}$ m$^{-3}$) using a combination of neutral beam injection and ICRH. The current ramp is continued to a flat top with an edge safety factor $q_{95}$ = 3.2 in a lower single null plasma configuration. The strike points are located close in corner of the horizontal and vertical plates of the divertor, where the pumping of the divertor cryopump is maximum. The power required to form an ITB's at 3.4 Tesla is above 18 MW for the scenario described. After ITB formation the core pressure continues to rise as can be seen from an increase in neutron rate ($R_{nt}$) and stored energy ($W_{dia}$) in Figure 1. The increase in pressure peaking leads in many cases to an internal kink instability and a subsequent disruption of the plasma at $\beta_N < 2$ [4]. The key to avoid these disruptions is a broading of the profiles. In Figure 2 the evolution $\beta_N$ versus density peaking ($n_{e0}/n_{e,average}$) is plotted. It is possible to avoid a continuous increase of the density peaking in discharges with an ITB by 1) transition to ELM free H-mode, which gives a rapid rise of the edge pedestal and 2) input power control to make a weaker barrier together with a control of the edge pedestal by impurity seeding. The three discharges in Figure 2 are at 3.4 Tesla, the maximum $\beta_N$ values obtained in the discharges that avoid a disruption is limited to $\beta_N$ ~2 at a maximum input power of 28 MW (18 MW NBI and 10 MW ICRH). In the following sections the evolution of ITB with an H-mode edge (section 3) and ITB discharges that use input power and edge control (section 4) are presented.

## 3. Internal Transport Barrier's and H-Modes

To illustrate what happens when an H-mode edge is added to a discharge with an internal transport barrier, pulse 39515 is described in detail. In this discharge the main heating is applied in 2 steps starting at 5 seconds with 8 MW NBI and a ramp up of the ICRF power to

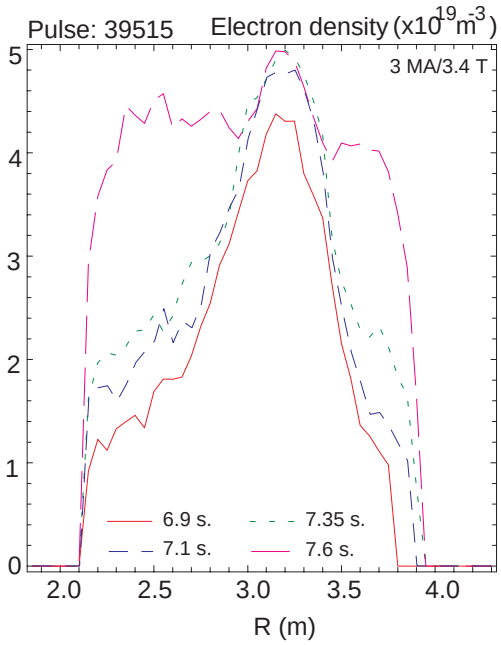


*Fig. 3. The evolution of the density profile, for a discharge with an ITB (pulse 39515), during the formation of the ELM free H-mode. At 6.9 seconds the ELM free H-mode starts. At 7.6 seconds the first ELM occurs.*

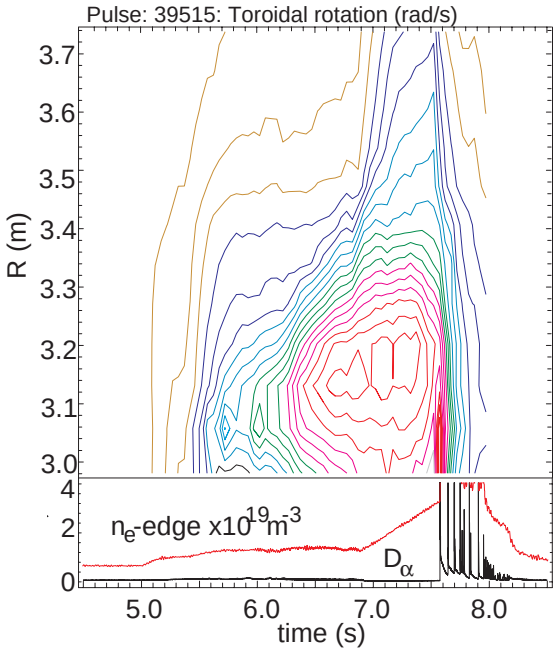


*Fig. 4. The formation of an ELM free H-mode in a discharge (pulse 39515) with an ITB, increases the edge rotation and hence decreases the rotation shear at the ITB location ($R_{ITB}$ = 3.4 m at 6.9 seconds).*

5 MW, at 5.5 seconds the NBI power is increased to 16 MW. At this stage the discharge is fuelled by NBI only and is similar to pulse 46664 of Figure 1. The internal barrier starts at 6.3 seconds, an ELM free H-mode forms at 6.9 seconds with type I ELM's starting from 7.6 seconds onwards. During this relatively long ELM free phase the edge density rises rapidly as is shown in Figure 3. Just before the start of the H-mode phase, the density profile is peaked, which evolves to a flat density profile during the ELM free period. In Figure 4, contours of constant toroidal rotation are plotted. Due to the improved edge confinement of the ELM free H-mode the rotation at the edge increases while the centre of the plasma remains at constant toroidal rotation. The decrease in rotation shear at the ITB location combined with a flattening of the density profile, leads to a weakening of the ITB at constant input power. In similar ITB discharges, measurement of the density fluctuations with reflectometry show a rapid increase of the fluctuation levels the at the ITB location, when the rotation at the edge increases [5].

After the ELM free phase, the measurement of the ion temperature by charge exchange spectroscopy (Figure 5) and the electron temperature from ECE measurements (Figure 6) show a rapid loss of the ITB at constant input power due to the ELM activity. These ELM's provoke a transient steepening of the gradients at the ITB location, due to a rapid loss of edge pressure. This is followed by an erosion of the temperature gradients and an inward movement of the ITB, as described in detail in [6]. In addition, the energy loss from the core increases ELM activity. This implies that an ITB and type I ELM form an intrinsically unstable combination, leading to towards a standard ELMy H-mode without an ITB [7]. An increase in the input power to try to keep the ITB is not possible since these discharge are close to the maximum input power available in JET.

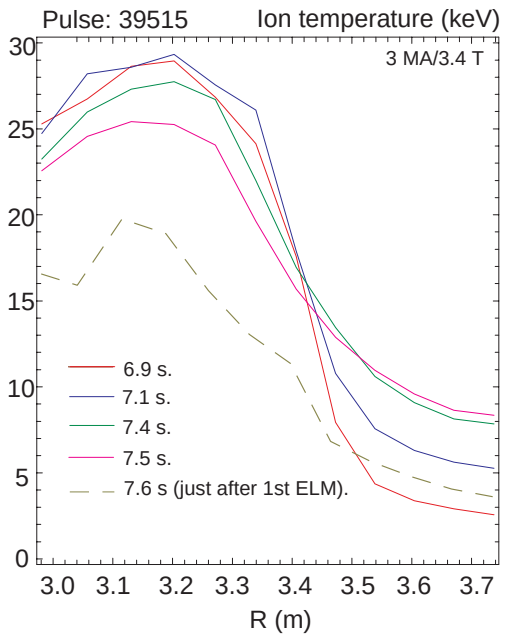


*Fig. 5. The ion temperature profiles after the start of an ELM free H-mode phase in an ITB discharge (pulse 39515). The ion temperature decreases strongly after the 1st type I ELM at constant input power.*

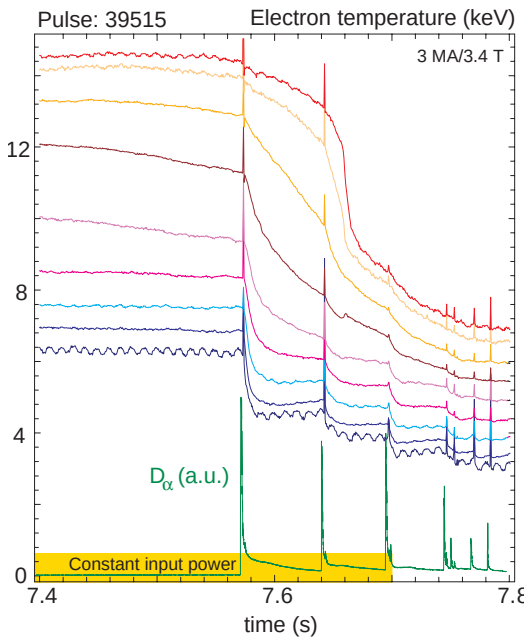


*Fig. 6. The electron temperature contours for the same discharge as in Fig. 5. The ITB weakens during the ELM free H-mode phase (before 7.58 seconds). The type I ELM's destroy the ITB at constant input power.*

An overview of high performance ITB discharges in Figure 7 indicates that this behavior is not unique to pulse 39515. A plot of the inverse ion-temperature scale length at the location of the ITB versus ion temperature at the edge of the plasma shows that an ITB can not be maintained at high edge temperature (edge pressures) observed during ELM free H-modes and ITB discharges with type I ELM's.

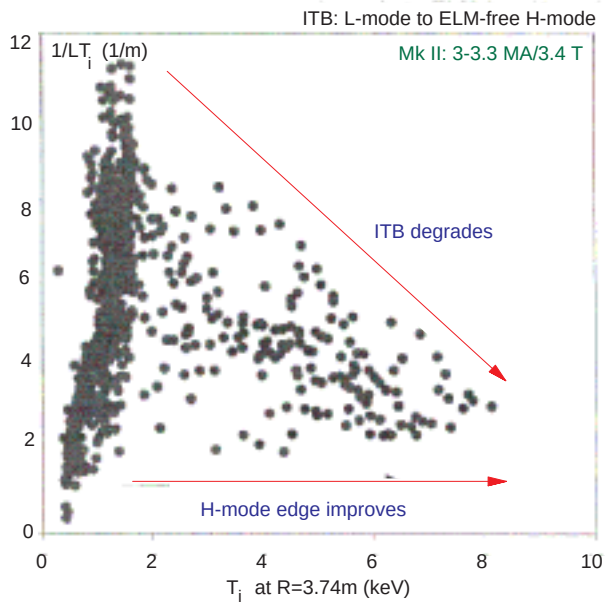


*Fig. 7. The inverse gradient length of the ion temperature at the ITB location plotted versus the ion temperature at the edge. The dataset shows that the core temperatures do not increase with the addition of an H-mode edge, rather the ITB is weaker for the cases with the highest edge pedestal temperatures [8].*

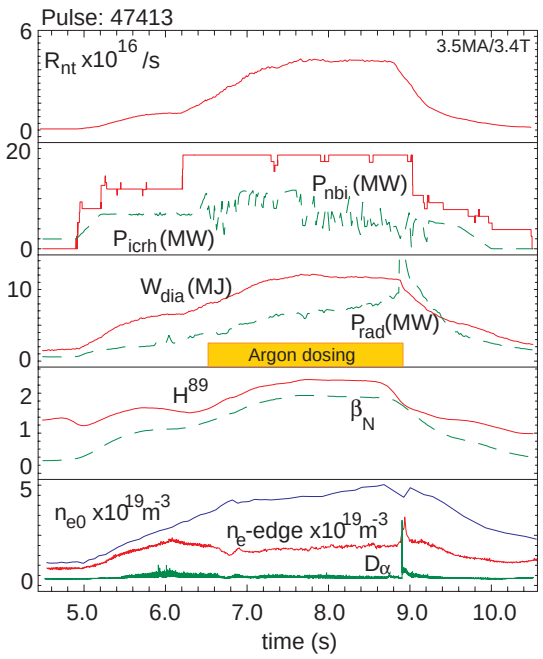


*Fig. 8. The formation and sustainment of a weaker ITB with control of the edge pedestal at 3.5MA/3.4T (pulse 47413). The weaker ITB is formed by delaying the high power phase and increasing the input power in steps. The edge is kept at low edge density with small ELM's by argon gas dosing. The ITB is formed at 6.1 seconds as can be seen from the increase in neutron rate ($R_{nt}$), stored energy ($W_{dia}$) and the peaking of the density profile. Note that during the argon dosing the radiated power ($P_{rad}$) rises to 30% of the input power. The edge density is kept constant at $2{\cdot}10^{19}$ m$^{-3}$.*

## 4. Sustain Weaker Internal Transport Barrier's with Edge Control

For ITB discharges, the edge of the plasma needs to be controlled to a lower, constant edge pressure than is typical for ELMy H-modes. This also implies that the control of the pressure profile need to be partly done by the input power, since the H-mode transport barrier at the edge can not be used to its full potential to broaden the pressure profile. By delaying the high power phase (higher central shear), and an increase of the input power in stages, a weaker ITB can be formed (see Figure 8). The control of the edge pressure can be achieved with impurity seeding. In the discharge shown in Figure 8, argon dosing is used to increase the radiation at the edge, enough to obtain small ELM's. The start of the argon dosing is timed with the step to maximum input power. During the argon dosing the radiation ($P_{rad}$) rises slowly to 30% of the input power, while the edge density is kept constant at $2{\cdot}10^{19}$ m$^{-3}$. The central density rises slowly to $5{\cdot}10^{19}$ m$^{-3}$, at maximum NBI power for 2.4 seconds, much less than the central NBI fuelling would allow (~$1{\cdot}10^{20}$ electrons$\cdot$m$^{-3}\cdot$s$^{-1}$ near the axis), and significantly less (< 50%) density rise compared to a 'strong' ITB (pulse 39515, Figure 3).

This result implies that an increase of the density has to be achieved with additional gas or pellet fuelling. Figure 9 gives a summary of ITB discharges at 3MA/3Tesla, with additional deuterium gas fuelling in combination with argon impurity seeding. The best steady ITB discharges are obtained without additional deuterium gas fuelling. Replacing the argon dosing by deuterium gas fuelling (pulse 47115 in Figure 9) leads to a rapid rise of the edge density and type I ELM activity, the ITB collapses. Maintaining the argon dosing during the deuterium gas fuelling (pulse 47110 in Figure 9) delays the start of the type I ELM activity, but a steady phase is not achieved. This indicates how important it is to keep the ELM's small and that for the input powers used the amount of argon dosing required needs to be carfully tuned. This is summarized in Figure 10 where the electron fuelling rate from the argon dosing is plotted against the neutron rate ($R_{nt}$) achieved; enough argon is needed to suppress the type I ELM activity, however too much argon leads to a decrease in the deuterium content of the plasma. In some cases too much argon drives the edge back to L-mode, which may lead to a disruption when the pressure profile becomes too peaked (similar limitation as described in section 2). An optimization of ITB discharges with different impurities has not been

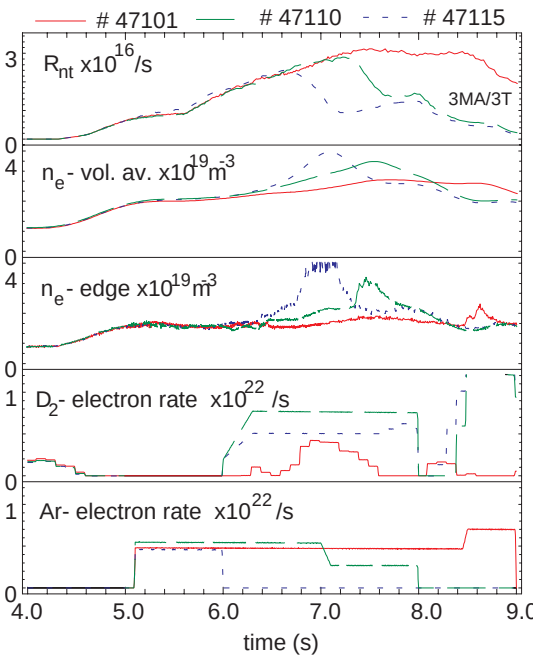


*Fig. 9. Three ITB discharges at 3MA/3T at the same input power (24 MW, not shown). The discharge (pulse 47101) at the lowest density sustains the ITB with argon dosing. Additional deuterium gas dosing (pulse 47110) or replacing the argon dosing with deuterium dosing (pulse 47115) lead to an increase in density, but in both cases the ITB collapses.*

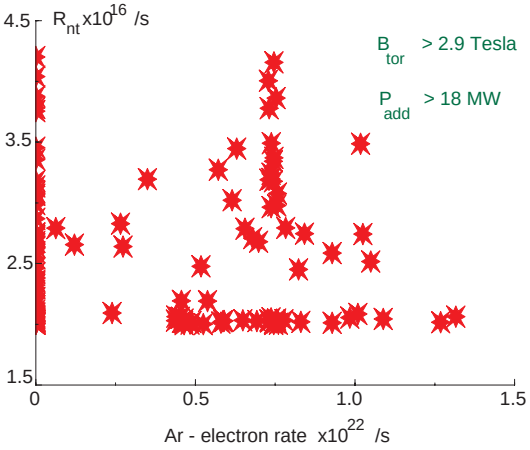


*Fig. 10. The amount of argon dosing applied in ITB discharges at $B_{tor}$ > 2.9 Tesla versus neutron rate ($R_{nt}$). The discharges without argon are transient ITB discharges. An optimum dosing rate is required to keep small ELM's without diluting the plasma too much.*

performed. Krypton gas dosing has also been used successfully to maintain small ELM's in JET. However, krypton accumulates in the vessel walls, giving difficulties to maintain the experimental conditions after only a few pulses.

Pellet fuelling of ITB discharges has been studied for a limited number of pulses. The pellet centrifuge system at JET has been used to inject pellets at 120-360 m/s into the edge of ITB discharges. The ablation of the pellet leads to a collapse of an ITB or the pellets prevent formation of the transport barrier when used early during the high power phase [7, 9]. The collapse of the ITB is similar to the collapse of the ITB during type I ELM's, however the pellet injection does allow some control on the timing of the pellet sequence. As described in [9], the most promising result show a reformation of the ITB ~1 second after pellet injection, allowing a possible optimization route for ITB's fuelled by a carefully timed string of pellets.

## 5. Confinement and Edge Conditions

The best ITB discharges in JET (transient and steady) are at low density. This implies, with the large heating power applied, a significant contribution (20% - 30%) of fast particles to the total stored energy ($W_{dia}$). H97 confinement enhancement factors calculated for the ITB discharges are plotted against the $n_{e,average}/n_{Greenwald}$ in Figure 11 and compared with standard H-mode discharges at 2.5MA/2.5T and $<\delta> = 0.35$ [10]. The ITB discharges with H97 in the range 1.2-1.6 are at significantly lower density (30 % $n_{e,average}/n_{Greenwald}$) compared to standard H-mode discharges and NBI fuelling alone with steady type I ELM's. Part of the improvement

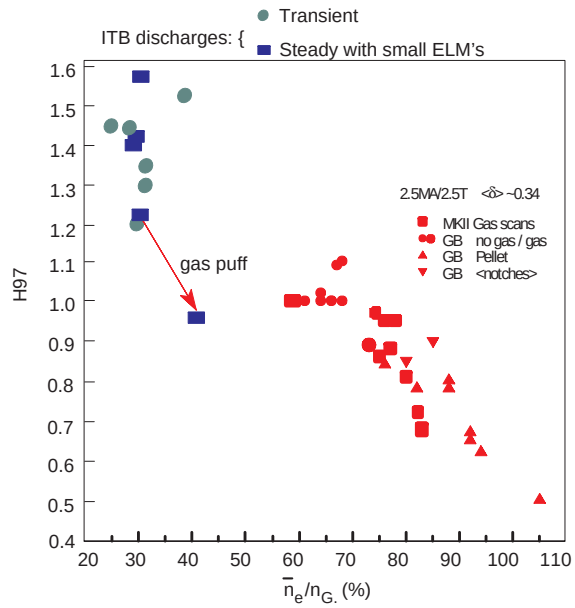


*Fig. 11. The H97 confinement enhancement versus Greenwald density fraction. The ITB discharges have good confinement compared to standard H-mode discharges at high density. However, part of the improvement comes from the density dependence of the scaling law applied, which is not observed in JET.*

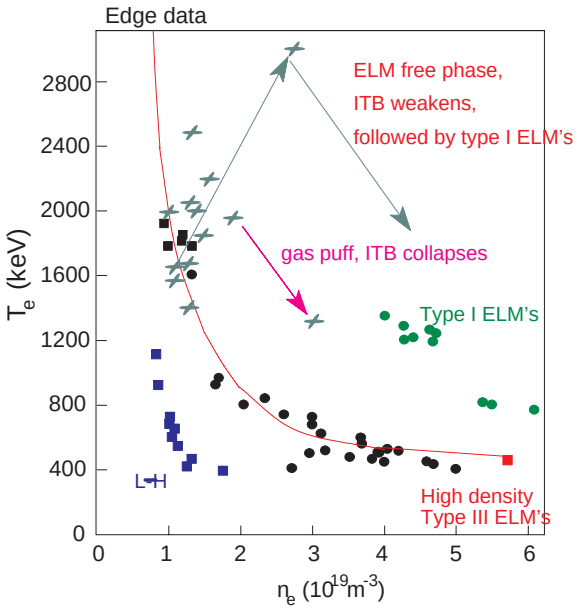


*Fig. 12. The edge electron temperature versus edge electron density. The ITB discharges are at low edge density close to the type III boundary. Indicated is the excursion of the edge to high density and type I ELM activity in ITB discharges with gas dosing or after the build up of the edge pedestal without argon dosing.*

of H97 values compared to standard H-modes is due to the $(n_{e,average})^{0.41}$ dependence of the confinement time in the scaling low, which is not observed in discharges in JET. However, the overall good confinement in ITB discharges is obtained with small ELM's; the contribution of the edge pedestal to the stored energy is less compared standard H-mode discharges.

ITB discharges maintain a peaked density profile (density peaking factors: 1.4-2.0) compared to flat density profiles for H-mode discharges. The average density in ITB discharges is typically 2-3 times lower compared to H-mode discharges. As a result, the edge density is much lower in ITB discharges and similar to L-mode discharges or discharges with type III ELM's, just after L-H mode transition, at low density. This is shown in an edge operational diagram, were the edge temperature is plotted against the edge density (Figure 12). The ITB discharges in JET are at lower pressure then the type I ELM discharges as stated above. In Figure 12 the evolution of a discharge with a transition to ELM free H-mode and a discharge with additional deuterium dosing are given. In these two discharges, the edge density rises and the edge parameters evolve towards the type I ELM region of the diagram, in both cases the ITB weakens and collapses with the onset of the ELM's.

The internal transport barrier has to be formed at low density to insure central power deposition at the barrier formation, and to avoid a rapid current penetration. After the formation of the ITB, the core temperatures are high enough to increase the density further. From the observation presented in this paper, a route to operation at high density with an ITB should follow the type III ELM boundary towards high edge density. This may be achieved

with a further optimization of the fuelling scenarios in combination with impurity gas dosing, or alternatively by establishing transport barriers at much lower input powers to avoid a transition to type I ELM's. In this respect the ITB's reported in [11] with LHCD preheating in JET are encouraging.

## 6. Conclusions

Internal transport barriers can be sustained in JET when combined with an edge pedestal controlled by small ELM's at low edge density. Good confinement is obtained in these discharges with H97 confinement enhancement factors 1.2-1.6 at line average densities around 30%-40% of the Greenwald density limit.

The operational space of the ITB regimes in JET is restricted to this low (edge) density. A route to operation at high density with an ITB should follow the type III ELM boundary towards high edge density in the edge operational diagram. This is supported by the observation that a strong increase in edge pressure during an ELM free H-mode weakens the transport barrier due to a reduction of the rotational shear and pressure profile at the ITB location. In addition, type I ELM activity, associated with a high edge pedestal pressure, lead to a collapse of the ITB with the input powers available in JET.

The increase in density toward reactor relevant densities may be achieved by an optimization of the deuterium fuelling scenarios and combination with impurity seeding in ITB scenarios used at present, or alternatively to have access to ITB's at lower input power in JET.

## References


[1] Gormezano, C., and the JET Team, "Optimization of JET Plasmas with Current Profile Control", Plasma Physics and Controlled Nuclear Fusion Research, Proc. 16th Int. Conf., Montreal, Vol I, IAEA Vienna, IAEA-CN-64/A5-5, (1996), 487-495.

[2] Sips, A.C.C., et al., "Operation at High Performance in Optimized Shear Plasmas in JET", Plasma Physics and Controlled Fusion 40 (1998), 1171-1184.

[3] Challis C.D., et al., "Conditions for Internal Transport Barrier Formation in JET", 26th EPS CCFPP, Maastricht, Vol. 23J (1999), 69-73

[4] Huysmans, G.T.A., et al., "MHD Stability Analysis of Optimised Shear Discharges in JET", 24th EPS CCFPP, Berchtesgaden (1997) Vol. 1 (1997) 21-24.

[5] Conway, G.D., et al., "Suppression of Plasma Turbulence During Optimized Shear Configurations in JET", Physical Review Letters, 84 (2000) 1463-1466.

[6] Sarazin, Y., et al., "Dynamics of ITB Perturbation due to Large ELM's in JET", 27th EPS CCFPP, Budapest (2000), CD-ROM file P1.050.

[7] Söldner, F.X., et al., "Optimised Shear Scenario Development on JET towards Steady-State", Plasma Physics and Controlled Fusion 39(12B) (1997) B353.

[8] Rochard, F., et al., "Characteristics of Internal Transport Barriers for the JET Optimised Shear Database", Cadarache Report EUR-CEA-FC-1677, submitted for publication in Nuclear Fusion (2000).

[9] Gormezano, C., et al., "Overview of JET Results in Support of the ITER Physics Basis", OV1/2, This conference.

[10] Sartori, R., et al., "Confinement Loss in JET ELMy H-modes", 26th EPS CCFPP, Maastricht (1999), 197-200.

[11] Challis C.D., et al., " The Effect of LHCD on the Evolution of Internal Transport Barriers in JET", 27th EPS CCFPP, Budapest (2000), CD-ROM file OR.019.